Inorg. Chem. **2007**, *46*, 10901–10906

Electrochemical and EPR Studies of the Corannulene Ruthenium(II) Sandwich Complex $[(\eta^6\text{-}C_6Me_6)Ru(\eta^6\text{-}C_{20}H_{10})](SbF_6)_2$

Robert J. Angelici and Bolin Zhu

Ames Laboratory and Department of Chemistry, Iowa State University, Ames, Iowa 50011-3111

Serena Fedi, Franco Laschi, and Piero Zanello*

Dipartimento di Chimica, Università di Siena, 53100, Siena, Italy

Received August 3, 2007

The dication $[(\eta^6\text{-}C_6Me_6)Ru(\eta^6\text{-}C_{20}H_{10})]^{2+}$ in propylene carbonate solution exhibits a sequence of reduction processes that is either metal-centered [Ru(II)/Ru(I)/Ru(0)] or ligand-centered. The marginally stable Ru(I) monocation $[(\eta^6\text{-}C_6Me_6)Ru(\eta^6\text{-}C_{20}H_{10})]^{+}$ has been characterized by EPR spectroscopy. The electrochemistry of $C_{20}H_{10}$ and EPR features of its stable monoanion $[C_{20}H_{10}]^{-}$ have also been revisited.

Introduction

Although corannulene $C_{20}H_{10}$ (Chart 1), which is the smallest curved subunit of C_{60},[1] has been known since 1967, only two short reports have dealt with its electrochemical properties[2] to the best of our knowledge. Buckminsterfullerene (C_{60}) undergoes up to six, chemically reversible, one-electron reductions[3] due to its triply degenerate LUMO. Since corannulene possesses a doubly degenerate LUMO,[4] it should also exhibit a rich electrochemistry. In fact, chemical reduction of corannulene (or its functionalized derivatives) has allowed the spectroscopic characterization of the −1, −2, −3, and −4 anions of corannulene.[1,4,5]

To date, there are no electrochemical studies of η^6-complexes of corannulene despite the fact that several have been synthesized.[6] Some of us recently reported the syntheses and crystal structures of a series of $[(\eta^6\text{-arene})M(\eta^6\text{-}C_{20}H_{10})]^{2+}$ (M = Ru, Os) complexes.[7] In particular, the dication $[(\eta^6\text{-}C_6Me_6)Ru(\eta^6\text{-}C_{20}H_{10})]^{2+}$ (Chart 1) proved to be notably stable, thus allowing us to investigate its electrochemical properties which we compare with those of corannulene itself.

Chart 1

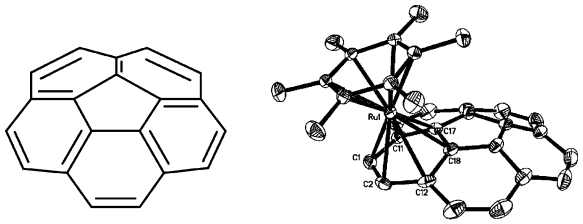

$C_{20}H_{10}$ $[(\eta^6\text{-}C_6Me_6)Ru(\eta^6\text{-}C_{20}H_{10})]^{2+}$, $\mathbf{1}^{2+}$

Experimental Section

The $[(\eta^6\text{-}C_6Me_6)Ru(\eta^6\text{-}C_{20}H_{10})](SbF_6)_2$ complex was prepared as previously reported.[7] Anhydrous 99.7% propylene carbonate (Aldrich) and anhydrous 98.5% nitromethane (Fluka) were used

* To whom correspondence should be addressed. E-mail: zanello@unisi.it.

(1) Aprahamian, I.; Preda, D. V.; Bancu, M.; Belanger, A. P.; Sheradaky, T.; Scott, L. T.; Rabinovitz, M. *J. Org. Chem.* **2006**, *71*, 290−298 and references therein.

(2) (a) Janata, J.; Gendell, J.; Ling, C.-Y.; Barth, W.; Backes, L.; Mark, H. B.; Lawton, R. G. *J. Am. Chem. Soc.* **1967**, *89*, 3056−3058. (b) Seiders, T. J.; Baldridge, K. K.; Siegel, J. S.; Gleiter, R. *Tetrahedron Lett.* **2000**, *41*, 4519−4522.

(3) (a) Ohsawa, Y.; Saji, T. *J. Chem. Soc., Chem. Commun.* **1992**, 781−782. (b) Xie, Q.; Pérez Cordero, E.; Echegoyen, L. *J. Am. Chem. Soc.* **1992**, *114*, 3978−3980. (c) Bubois, D.; Moninot, G.; Kutner, W.; Jones, M. T.; Kadish, K. M. *J. Phys. Chem.* **1992**, *96*, 7137−7145.

(4) (a) Baumgarten, M.; Gherghel, L.; Wagner, M.; Weitz, A.; Rabinovitz, M.; Cheng, P.-C.; Scott, L. T. *J. Am. Chem. Soc.* **1995**, *117*, 6254−6257 and references therein. (b) Rabideau, P. W.; Marcinov, Z.; Sygula, R.; Sygula, A. *Tetrahedron Lett.* **1993**, *40*, 6351−6354. (c) Zilber, G.; Rozenshtein, V.; Cheng, P.-C.; Scott, L. T.; Rabinovitz, M.; Levanon, H. *J. Am. Chem. Soc.* **1995**, *117*, 10720−10725.

(5) Shabtai, E.; Hoffman, R. E.; Cheng, P.-C.; Preda, D. V.; Scott, L. T.; Rabinovitz, M. *J. Chem. Soc., Perkin Trans. 2* **2000**, 129−133.

(6) (a) Seiders, T. J.; Baldridge, K. K.; O'Connor, J. M.; Siegel, J. S. *J. Am. Chem. Soc.* **1997**, *119*, 4781. (b) Vecchi, P. A.; Alvarez, C. M.; Ellern, A.; Angelici, R. J.; Sygula, A.; Sygula, R.; Rabideau, P. W. *Organometallics* **2005**, *24*, 4543. (c) Vecchi, P. A.; Alvarez, C. M.; Ellern, A.; Angelici, R. J.; Sygula, A.; Sygula, R.; Rabideau, P. W. *Angew. Chem., Int. Ed.* **2004**, *43*, 4497. (d) Alvarez, C. M.; Angelici, R. J.; Sygula, A.; Sygula, R.; Rabideau, P. W. *Organometallics* **2003**, *22*, 624. (e) Siegel, J. S.; Baldridge, K. K.; Linden, A.; Dorta, R. *J. Am. Chem. Soc.* **2006**, *128*, 10644−10645. (f) Wu, Y.-T.; Siegel, J. S. *Chem. Rev.* **2006**, *106*, 4843.

(7) Zhu, B.; Ellern, A.; Sygula, A.; Sygula, R.; Angelici, R. J. *Organometallics* **2007**, *26*, 1721.

10.1021/ic7015512 CCC: $37.00
Published on Web 11/14/2007

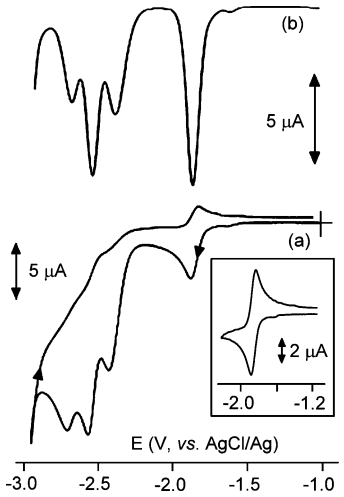

Figure 1. Cyclic (a) and Osteryoung square wave (b) voltammetric responses recorded at a mercury electrode in a PC solution of $C_{20}H_{10}$ (1.1×10^{-3} M). $[NBu_4][PF_6]$ (0.2 M) supporting electrolyte. Scan rates: (a, inset) 0.2 V s^{-1}; (b) 0.1 V s^{-1}. $T = 253$ K.

as received. Anhydrous 99.9% HPLC-grade tetrahydrofuran (Aldrich) was distilled in the presence of sodium before use. Fluka $[NBu_4][PF_6]$ (electrochemical grade) was used as the supporting electrolyte (0.2 M).

Cyclic voltammetry was performed in a three-electrode cell containing the working electrode surrounded by a platinum-spiral counter electrode, and the reference electrode was mounted with a Luggin capillary. For low-temperature measurements, the central part of the cell (nonisothermal assembly) was enclosed by a thermostatic jacket through which a cooled liquid was circulated.

At room temperature the reference electrode was an aqueous saturated calomel electrode (SCE); at low temperature, a Ag/AgCl electrode, filled with the solution under investigation, was used. Platinum, gold, mercury, and glassy carbon were used as materials for the working electrodes. A BAS 100W electrochemical analyzer was used as the polarizing unit. All potential values are referred to the Ag/AgCl reference electrode. Under the present experimental conditions and at 293 K, the one-electron oxidation of ferrocene occurs at $E^{\circ\prime} = +0.33$ V in propylene carbonate, $E^{\circ\prime} = +0.49$ V in tetrahydrofuran, and $E^{\circ\prime} = +0.34$ V in nitromethane.

Controlled potential coulometry was performed in an H-shaped cell with anodic and cathodic compartments separated by a sintered-glass disk. The working microelectrode was a platinum gauze or mercury pool; a mercury pool was used as the counter electrode.

Electron spin resonance (ESR) spectra were recorded with a ER 200 D-SRC Bruker spectrometer operating at X-band frequencies using a HS Bruker rectangular cavity. Control of the operational frequency was achieved with a Hewlett-Packard X5−32 B wavemeter, and the magnetic field was calibrated with the DPPH (1,1-diphenyl-2-picrylhydrazyl) radical as a suitable field marker. Control of the temperature was achieved with a Bruker ER 4111 VT device (±1 K). The g values are referred to the external standard reference DPPH ($g = 2.0036$).

Results and Discussion

Corannulene ($C_{20}H_{10}$). In order to understand the redox chemistry of $[(\eta^6\text{-}C_6Me_6)Ru(\eta^6\text{-}C_{20}H_{10})]^{2+}$, it was necessary to study the voltammetric behavior of $C_{20}H_{10}$ in propylene carbonate (PC) solution at low-temperature (Figure 1). The first reduction of $C_{20}H_{10}$ has features of chemical reversibility on the cyclic voltammetric time scale. It is followed by three additional essentially irreversible reduction processes. Controlled potential coulometry ($E_w = -2.0$ V) for the first reduction exhibits fast consumption of about one-electron per $C_{20}H_{10}$ molecule, but the electrolysis current continues slowly probably because of fast reoxidation by traces of air. Nevertheless, based on previous electrochemical[2] and chemical[4] studies as well as on a comparison of the peak height of the cyclic voltammetric response with that of an equimolar solution of ferrocene (Figure S1 in Supporting Information), we confidently assign the first reduction to a one-electron process.[8]

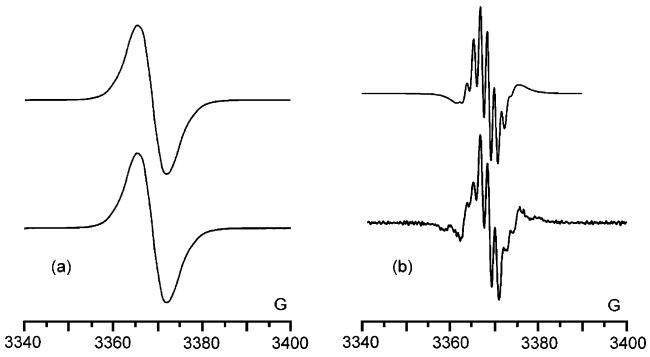

Figure 2. X-band EPR spectrum of $[C_{20}H_{10}]^-$ in PC glassy solution at $T = 103$ K. (a) Experimental (bottom) and simulated (top) first-derivative mode; (b) experimental (bottom) and simulated (top) third-derivative mode. $\nu = 9.456$ GHz.

Analysis of the cyclic voltammetric responses at scan rates that increase from 0.02 to 2.00 Vs^{-1} shows that the one-electron process $C_{20}H_{10}/[C_{20}H_{10}]^-$ is chemically and electrochemically reversible in the temperature range from 253 to 293 K, which is consistent with the previously established stability of the monoanion[2a,4] and also suggests that no significant structural change accompanies the one-electron addition. In contrast to the first reduction, subsequent reductions to the di-, tri-, and tetracorannulene anions are accompanied by fast chemical complications, which means that they are very short lived under our experimental conditions.

The di-and trianions arising from the chemical reduction of corannulene with alkaline metals in THF solution have been previously characterized spectroscopically. On the short time scale of these reductions, only the tetraanion generation using lithium was complicated by dimerization.[1,4,5] Detection of four separate reduction steps for corannulene on the longer electrochemical time scale of our present studies is consistent with results from the chemical reductions.[1,4,5]

In tetrahydrofuran solution, a chemically reversible first reduction is also observed. However, the second and third irreversible reductions merge with each other, whereas the fourth reduction possesses features of partial chemical reversibility (Figure S2 in Supporting Information). Previous electrochemical investigations in acetonitrile solution only mention the occurrence of two reductions.[2] Electrode po-

(8) This conclusion is based on the reliable assumption that these molecules have similar diffusion coefficients (MWs: 240 vs 186), see: Zanello, P. *Inorganic Electrochemistry. Theory, Practice and Application*; Royal Society of Chemistry: UK, 2003.

Table 1. Formal Electrode Potentials (V vs Ag/AgCl) and Peak-to-Peak Separations (mV) for the Redox Processes Exhibited in Different Solvents and at Different Temperatures (K) by $C_{20}H_{10}$ (Mercury Working Electrode), $[(\eta^6\text{-}C_6Me_6)Ru(\eta^6\text{-}C_{20}H_{10})]^{2+}$, $\mathbf{1}^{2+}$, and the Related $[(\eta^6\text{-}C_6Me_6)_2Ru)]^{2+}$, $\mathbf{2}^{2+}$ (Mercury or Gold Working Electrodes), and C_{60}

	corannulene reductions					Ru(II)-centered reductions				
complex	$E°$ (first reduction)	ΔE_p[a]	E_p[b] (second reduction)	E_p[b] (third reduction)	E_p[b] (fourth reduction)	$E°_{II/I}$[b]	$E°_{I/0}$[b]	$\Delta E°$ [c]	solvent	T, K
$C_{20}H_{10}$	−1.86	54	−2.40	−2.56	−2.70				PC	253
	−1.90	71	−2.42	−2.57	d				PC	273
	−1.91	70	−2.43	−2.58	d				PC	290
	−2.02	340	−2.85	−2.85	−3.09				THF	253
	−1.88[e]		−2.36[e]						MeCN	
	−1.86[f]		−2.43[f]						MeCN	
$\mathbf{1}^{2+}$	−2.27[b,g]		−2.40[b,g]	−2.63[b,g]	h	−0.39	−0.42	0.06	PC	253
	−2.24[b,g]		−2.37[b,g]	−2.61[b,g]	−2.70[b,g]	−0.37	−0.45	0.08	PC	273
	−2.28[b,g]		−2.41[b,g]	−2.62[b,g]	−2.71[b,g]	−0.35	−0.44	0.09	PC	290
						−0.39	−0.50	0.11[b]	$MeNO_2$	253
						−0.36	−0.47	0.11[b]	$MeNO_2$	273
						−0.37	−0.48	0.11[b]	$MeNO_2$	290
$\mathbf{2}^{2+}$ [i,j]						−0.92	−1.08	0.16	CH_2Cl_2	298
						−0.98	−0.98	0	MeCN	298
C_{60}	−0.46[b,j]		−0.88[b,j]	−1.36[b,j]	−1.78[b,j]				PC−CH_2Cl_2 (3:1)	290

[a] Measured at 0.2 V s^{-1}. [b] From Osteryoung square wave voltammetry (OSWV) at 0.1 V s^{-1}. [c] From cyclic voltammetry at 0.2 V s^{-1} according to ref 13. [d] Partially overlapped by the third reduction. [e] From ref 2a. [f] From ref 2b. [g] Peak potential values. [h] Not possible to determine. [i] From ref 12. [j] Platinum electrode.

Table 2. Temperature-Dependent X-band EPR Parameters for the Species $[\mathbf{1}]^+$ and $[C_{20}H_{10}]^-$ [a]

complex	g_l	g_m	g_h	$\langle g\rangle$	g_{iso}	a_l	a_m	a_h	a_{iso}	$\langle a\rangle$	δg_{l-h}	solvent
$\mathbf{1}^+$	2.086	1.989	1.942	2.006		≤11.0[b]	≤8.0[b]	≤11.0[b]		≤10.0[b]	0.144	PC[c]
$[C_{20}H_{10}]^-$	2.0045	2.0045	2.0045	2.0045	2.0037	1.5	1.5	1.5	1.5	1.5	≤5.6[b]	PC[c]
					2.00270				1.560			DME[d]
					2.0027				1.57			THF[e]

[a] $\langle g\rangle = 1/3(g_l + g_m + g_h)$; $\langle a\rangle = 1/3(a_l + a_m + a_h)$; $g_i[\mathbf{1}]^+ = \pm 0.008$; $g_i[C_{20}H_{10}]^- = \pm 0.0008$; $a_i[\mathbf{1}]^+ = \pm 5$ G; $a_i[C_{20}H_{10}]^- = \pm 0.2$ G; $\Delta H_i[\mathbf{1}]^+ = \pm 4$ G; $\Delta H_i[C_{20}H_{10}]^- = \pm 0.1$ G) [b] From digital simulation. [c] Present work. [d] From ref 2a. [e] From ref 4.

tential values in different solvents are compiled in Table 1 together with values for $(\eta^6\text{-}C_6Me_6)Ru(\eta^6\text{-}C_{20}H_{10})^{2+}$, which will be discussed in the next section. Also included in this table are formal electrode potentials for the reversible reductions of C_{60}. Because of its insolubility in PC, the electrochemical data for C_{60} were obtained in PC−CH_2Cl_2 (3:1) solution.

Since the EPR spectrum of the chemically prepared $[C_{20}H_{10}]^-$ monoanion was reported only at room temperature,[2a,4] we recorded it at 103 K after its electrogeneration at low temperature (253 K) in PC solution (Figure 2). The experimental line shape can be suitably simulated assuming a $S = {}^1/_2$ electron spin Hamiltonian with spectral resolution in a pseudo-isotropic symmetry. The relatively broad and nearly unresolved first-derivative spectrum displays very weak anisotropic features in the rigid limit conditions ($\Delta H_{exp} \geq \Delta g_i$). The second- and third-derivative line shape analysis allows us to better characterize the hyperfine (hpf) structure expected for a highly symmetric organic radical. This hpf structure arises from paramagnetic coupling of the unpaired electron with the 10 equivalent protons of the anion (the ^{13}C signals are not detectable due to its low natural abundance).[9,10] In fact, 11 ^1H hpf signals are expected ($S = 1/2$, I_{tot} (^1H) = 10 × $^1/_2$ = 5) with relative intensities of 1:10:45:120:210:252:210:120:45:10:1. The multiple derivative simulation procedure[11] reveals the presence of 9 ^1H hpf features but fails to detect the outer absorptions (low and high field, relative intensities = 1:10). Nevertheless, the fourth and fifth derivatives show the presence of such low-intensity signals with slight asymmetry.

The simulation also reveals the role of the different α, β, γ, δ, ... line width contributions to the overall ΔH_{exp} expression.[9,10]

$$\Delta H(m_i) = \alpha + \beta(m_{Ii}) + \gamma(m_{Ii}^2) + \delta(m_{Ii}^3) + ... \qquad (1)$$

On the basis of the pertinent contributions, the best fit line width parameters are[11] α = 2.42 (0.05) G, β = −0.10 (0.01) G, and γ = 0.07 (0.01) G. The $|\alpha/\beta|$ ratio > 1 (namely, $|\alpha/\beta|$ = 24.2) indicates a low degree of asymmetry for the monoanion SOMO and confirms that its geometric skeleton is basically symmetric.[9]

At the glassy−fluid transition (218 K), the anisotropic broad spectrum transforms into a narrow isotropic signal because of a significant reduction in the experimental line width under fast motion conditions. However, the signal rapidly vanishes due to the chemical reactivity of the radical

(9) Mabbs, E.; Collison, D. Electron Paramagnetic Resonance of d Transition Metal Compounds. *Studies in Inorganic Chemistry*; Elsevier: New York, 1992; Vol. 16.
(10) Drago, R. S. *Physical Methods for Chemists*; Saunders College Publishers: New York, 1992.
(11) (a) Lozos, G. P.; Hoffman, B. M.; Franz, C. G. *Quantum Chem. Program Exchange* **1974**, *11*, 265. (b) Della Lunga, G. *ESRMGR Simulation Program Package*; Department of Chemistry, University of Siena: Siena, Italy 1998.

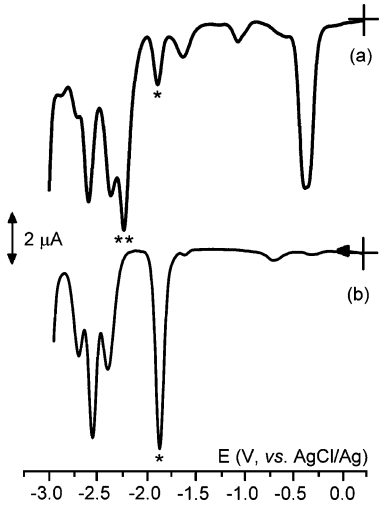

Figure 3. Osteryoung square wave voltammetric responses recorded at a mercury electrode in PC solutions: (a) $[(\eta^6\text{-}C_6Me_6)Ru(\eta^6\text{-}C_{20}H_{10})](SbF_6)_2$ (1.2×10^{-3} M); (b) $C_{20}H_{10}$ (1.1×10^{-3} M). $[NBu_4][PF_6]$ (0.2 mol dm^{-3}) supporting electrolyte. Scan rate 0.1 V s^{-1}. $T = 253$ K.

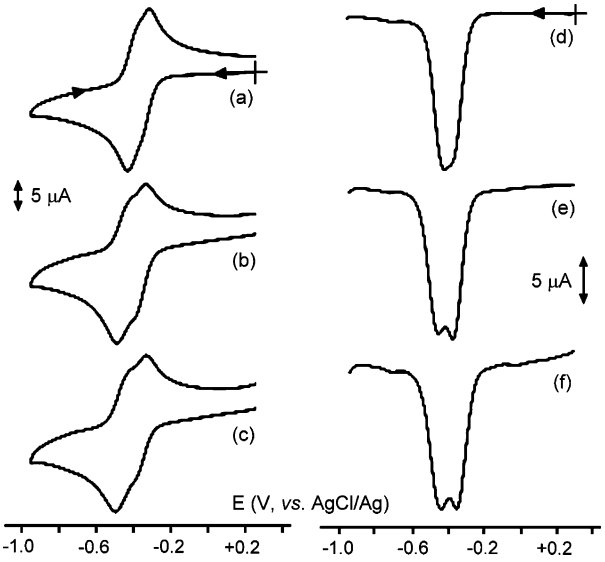

Figure 4. Cyclic (a−c) and Osteryoung square wave (d−f) voltammograms recorded at a mercury electrode in PC solution of $[(\eta^6\text{-}C_6Me_6)Ru(\eta^6\text{-}C_{20}H_{10})](SbF_6)_2$ (1.2×10^{-3} M). $[NBu_4][PF_6]$ (0.2 M) supporting electrolyte. Scan rates: (a−c) 0.2 and (d−f) 0.1 V s^{-1}. $T =$ (a,d) 253 K, (b,e) 273 K, and (c,f) 290 K.

monoanion in the presence of air. The experimental isotropic parameters g_{iso} and a_{iso} agree well with the corresponding pseudo-isotropic parameters in frozen solution, thus confirming that the highly symmetric geometry of the monoanion is maintained under different experimental conditions. The temperature-dependent EPR parameters of the corannulene monoanion are summarized in Table 2 together with those of the Ru(I) monocation $[(\eta^6\text{-}C_6Me_6)Ru(\eta^6\text{-}C_{20}H_{10})]^+$, which is discussed below. Previous results on the room-temperature EPR characterization of $[C_{20}H_{10}]^-$ in dimethoxyethane (DME) or THF solution[2a,4] agree well with those of the present study.

$[(\eta^6\text{-}C_6Me_6)Ru(\eta^6\text{-}C_{20}H_{10})]^{2+}$. The electrochemistry of $[(\eta^6\text{-}C_6Me_6)Ru(\eta^6\text{-}C_{20}H_{10})](SbF_6)_2$ was investigated in either nitromethane or propylene carbonate, but since nitromethane displays a limited cathodic window (because of the $NO_2/NO_2^{\bullet-}$ reduction), most of these studies were performed in propylene carbonate solution. Figure 3 shows the overall Osteryoung square wave voltammetric profile (a) of the Ru(II) complex along with that of free corannulene (b). Except for the reduction process at about −0.5 V, which belongs to the Ru(II) center and will be discussed in detail below, it is reasonable to assume that the double-asterisked peak in Figure 3a is due to the first corannulene-centered reduction, which is cathodically shifted as compared with that of corannulene by about 0.4 V upon coordination to the {Ru(C_6Me_6)} fragment. The fact that the further reductions of corannulene do not undergo an appreciable shift to more negative potential values seems to suggest that chemical complications following the Ru-centered reductions (see below) afford minor amounts of free corannulene (single-asterisked peak) and unidentified byproducts, as indicated by the minor reduction peaks present in the range from −0.5 to −1.7 V.

Studies of the first reduction process of the complex at different scan rates and temperatures are shown in Figure 4. Two rather close reductions are detected, which, in spite of apparent chemical reversibility at relatively high scan rates, reveal the presence of chemical complications at low scan rates (<0.1 V s^{-1}). Such voltammetric behavior is quite similar to that recorded for $[(\eta^6\text{-}C_6Me_6)_2Ru)]^{2+}$ in CH_2Cl_2 solution,[12] which suggests that the two reductions of the complex may be assigned to the two processes in the sequence Ru(II)/Ru(I)/Ru(0). In fact, controlled potential coulometry ($E_w = -0.7$ V) carried out at 273 K shows the consumption of about 1.4−1.5 electrons per molecule, which indicates a relatively fast decomposition of the complex after the first reduction step. As a consequence of this decomposition, the original intense yellow solution turns yellow red and the voltammetric profile of free corannulene is recorded.

A similar behavior was recorded in nitromethane solution for the Ru(II)/Ru(I)/Ru(0) sequence, but at more cathodic potentials the voltammetric profile is obscured by the redox activity of the solvent. It is noted that in this solvent the two reductions appear to be slightly more separated and the kinetics of the decomposition following the Ru(I)/Ru(0) step seems more sensitive to the temperature than in PC (Figure S3, Supporting Information). The magnitude of the splitting between the two reductions was noted to be dependent on the solvent also for $[(\eta^6\text{-}C_6Me_6)_2Ru)]^{2+}$; these reductions are separated in CH_2Cl_2 but simultaneous in MeCN.[12] The formal electrode potentials of the redox changes exhibited by $[(\eta^6\text{-}C_6Me_6)Ru(\eta^6\text{-}C_{20}H_{10})]^{2+}$ are compiled in Table 1 along with those of $[(\eta^6\text{-}C_6Me_6)_2Ru)]^{2+}$ and free corannulene.

It is evident that the Ru(II)−corannulene dication $\mathbf{1}^{2+}$ undergoes reduction at potential values markedly less negative than the Ru(II)−hexamethylbenzene dication $\mathbf{2}^{2+}$. This difference may be attributed not only to the lack of the electron-donating methyl groups on the $\eta^6\text{-}C_6$ ring of the corannulene ligand as compared with $\eta^6\text{-}C_6Me_6$ but also to

(12) Pierce, D. T.; Geiger, W. E. *J. Am. Chem. Soc.* **1992**, *114*, 6063−6073.
(13) Richardson, D. E.; Taube, H. *Inorg. Chem.* **1981**, *20*, 1278.

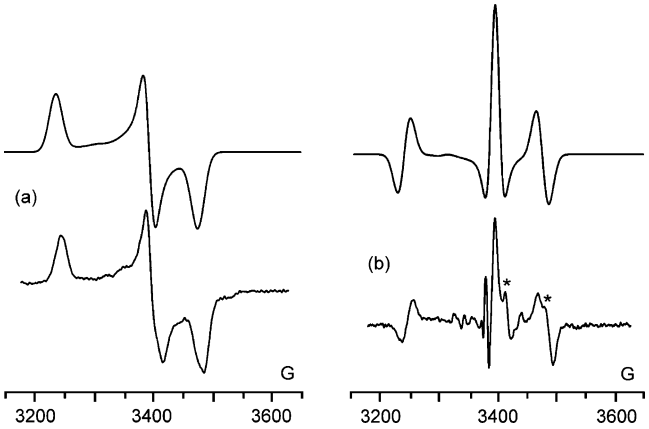

Figure 5. X-band EPR spectrum of $[(\eta^6\text{-}C_6Me_6)Ru(\eta^6\text{-}C_{20}H_{10})]^+$ in PC solution at 103 K. (a) Experimental (bottom) and simulated (top) first-derivative mode; (b) experimental (bottom) and simulated (top) second-derivative mode. $\nu = 9.450$ GHz.

the extended electronic delocalization of the corannulene, which acts as an electron-withdrawing group on the Ru(II) center.

In spite of the limited chemical reversibility of the Ru(II)/Ru(I)/Ru(0) sequence, we carried out the controlled potential stepwise reduction of $\mathbf{1}^{2+}$ in PC ($E_w = -0.6$ V) solution and recorded the EPR spectra. In order to decrease further the inherently slow chemical complications accompanying the Ru(II)/Ru(I) process, the macroelectrolysis was carried out at 250 K. Figure 5 shows the low-temperature X-band EPR spectrum of the monocation $[(\eta^6\text{-}C_6Me_6)Ru(\eta^6\text{-}C_{20}H_{10})]^+$ generated in the first stages of the reduction process (i.e., after consumption of about 0.3 electrons/molecule). The $\mathbf{S} = {}^1/_2$ electron spin Hamiltonian accounts for the three intense and well-separated rhombic signals arising from a low-spin Ru(I) center in the presence of strong field ligands.[9,10] The multiple derivative analysis reveals the larger line width of the anisotropic absorptions with respect to those of the ligand itself. Accordingly, the first-derivative experimental line width overlaps significantly the underlying hyperfine (hpf) couplings of the naturally occurring ruthenium isotopes (^{99}Ru, $I = 5/2$, natural abundance = 12.7%; ^{101}Ru, $I = 5/2$, natural abundance = 17%) and the ^{1}H nuclei superhyperfine (shpf) couplings (if any) of the two ligands. On the basis of the simulation procedure, an upper limit for such magnetic interactions can be proposed as $\Delta H_i \geq a_i(^1H)$.

As expected, the g_i values differ significantly from those of the free electron ($g_{electron} = 2.0023$). This proves that the 4d−Ru(I) spin orbit coupling (λ_{SO} coupling constant = 900 cm^{-1}) contributes substantially to the experimental anisotropic line shape of the complex and the related SOMO.[9] The relevant computed parameters are collected in Table 2.

The absence of ^{1}H hyperfine features associated with the well-resolved rhombic line shape emphasizes the importance of the ligand symmetry experienced by the unpaired spin density. In fact, $S = {}^1/_2$ paramagnetic systems under rigid limit conditions display different anisotropic spectral behavior (i.e., from pseudo-isotropic to axial to rhombic symmetry resolution) that is strongly dependent on the geometric symmetry of the overall SOMO, which depends on the more or less symmetric features of the ligand field.[14] In the present case, the rhombic spectral pattern reflects well the unsymmetrical coordinating mode of the corannulene ligand to the Ru(I)−C_6Me_6 moiety. In addition, the significant anisotropic line widths testify to the role of Ru(I) orbital contributions to the overall SOMO.

It is noted that the second- and third-derivative spectra allow us to detect the presence of two further minor signals (asterisked peaks), which overlap the g_m and g_h high-field features. The respective paramagnetic features (g_i anisotropies and ΔH_i) suggest that they can be attributed to byproducts arising from fragmentation of the reliably electrogenerated Ru(I) monocation. The amounts of such byproducts increase to the detriment of the three rhombic signals during controlled potential electrolysis.

Increasing the temperature to the glassy−fluid transition causes the anisotropic signal to disappear, and the fluid solution becomes EPR mute. In agreement with the instability of $[(\eta^6\text{-}C_6Me_6)Ru(\eta^6\text{-}C_{20}H_{10})]^+$, the EPR spectrum of a refrozen solution shows no evidence for the original rhombic Ru(I) features; instead, a number of broad and unresolved signals due to radical species resulting from complete fragmentation of the monocation is observed.

Conclusions

The first electrochemical investigation of an η^6-corannulene complex, namely, $[(\eta^6\text{-}C_6Me_6)Ru(\eta^6\text{-}C_{20}H_{10})]^{2+}$, is reported. In different nonaqueous solvents it undergoes two very close, one-electron reductions at about −0.5 V (vs AgCl/Ag), which possess features of chemical reversibility on the short time scale of cyclic voltammetry but are accompanied by slow chemical complications on the longer time scale of exhaustive electrolysis. Low-temperature (103 K) EPR spectroscopy indicates that the overall process is attributable to the Ru(II)/Ru(I)/Ru(0) sequence of reductions. The electrogenerated monocation $[(\eta^6\text{-}C_6Me_6)Ru(\eta^6\text{-}C_{20}H_{10})]^+$ exhibits three rhombic EPR absorptions, which not only agrees with the overall geometric asymmetry of the complex but can be nicely simulated taking into account the presence of 4d−Ru(I) spin orbit coupling. Among the byproducts generated by the partial chemical reversibility of the Ru(II)-centered reductions is free corannulene. A comparison with $[(\eta^6\text{-}C_6Me_6)_2Ru)]^{2+}$ shows that the Ru(II)/Ru(I)/Ru(0) sequence is thermodynamically more favorable in the corannulene complex (by about 0.5 V), probably because of the electron-withdrawing effect exerted by the extended electronic unsaturation of corannulene. The slowness of the chemical complications allows us to observe a one-electron reduction of the $C_{20}H_{10}$ ligand in the residual $[(C_6Me_6)Ru(C_{20}H_{10})]$ at potentials more negative by about 0.4 V with respect to free corannulene (−2.3 V vs −1.9 V). We also revisited the electrochemistry of free corannulene, confirming qualitatively the previously reported chemical reductions to $[C_{20}H_{10}]^{-/2-/3-/4-}$. On the time scale of the electrochemical

(14) Diversi, P.; Fontani, M.; Fuligni, M.; Laschi, F.; Matteoni, S.; Pinzino, C.; Zanello, P. *J. Organomet. Chem.* **2001**, *626*, 145.

reductions, the multiply charged anions are not sufficiently stable to be detected by common spectroscopic procedures. However, we determined the EPR features of $[C_{20}H_{10}]^-$ under glassy conditions.

Acknowledgment. P.Z. gratefully acknowledges the financial support of the University of Siena (PAR Progetti 2005). Partial support of this project was provided by the U.S. Department of Energy under contract DE-AC02-07CH11358 with Iowa State University. We are grateful to Drs. Andrzej and Renata Sygula, Mississippi State University, for a gift of corannulene.

Supporting Information Available: Cyclic voltammetric response of $C_{20}H_{10}$ with respect to that of an equimolar amount of $Fe(C_5H_5)_2$ in PC solution; cyclic voltammograms of $C_{20}H_{10}$ in THF solutions and $[(\eta^6\text{-}C_6Me_6)Ru(\eta^6\text{-}C_{20}H_{10})](SbF_6)_2$ in $MeNO_2$ solution. This material is available free of charge via the Internet at http://pubs.acs.org.

IC7015512